Sequence and Structure of the Membrane-Associated Peptide of Glycophorin A†

Najib Challou,‡ Erik Goormaghtigh,‡ Véronique Cabiaux,‡ Karel Conrath,§ and Jean-Marie Ruysschaert*,‡

Laboratoire de Chimie Physique des Macromolécules aux Interfaces, CP 206/2, Free University Brussels, Bd du triomphe, 1050 Brussels, Belgium, and Protein Chemistry, Smith Kline Beecham Biologicals, 89 rue de l'Institut, Rixensart, Belgium

Received January 25, 1994; Revised Manuscript Received March 16, 1994®

ABSTRACT: Glycophorin A (GPA) has been reconstituted into dimyristoylphosphatidylcholine vesicles and digested with proteinase K to identify the membrane domain and to characterize its structure and orientation. After digestion of the inner and outer domain of GPA by protease action restricted to the aqueous phase, a protected peptide migrates on an electrophoresis gel as a 7.5-kDa dimer (His^{66}–Ile^{95}). The secondary structure and orientation in a lipid bilayer of the 7.5-kDa dimer have been studied by Fourier transform infrared spectroscopy. Our proteolytic and spectroscopic data are in agreement with a topological model in which the His^{66}–Glu^{72} peptide adopts a β-sheet conformation and is oriented parallel to the lipid–water interface and the Ile^{73}–Ile^{95} domain is helical and oriented parallel to the lipid acyl chains, in a transmembrane configuration. Digestion of the domain protruding to the outside of the liposome generates "head–head" and "head–tail" dimers of 16 and 38 kDa, respectively. This observation is discussed in terms of the specificity of the dimer formation process.

Glycophorin A (GPA),[1] the major sialoglycoprotein of the human erythrocytes, is made of a single polypeptide chain of 131 amino acids (Tomita et al., 1978) and 16 oligosaccharide chains which form 60% of its weight. The proposed topology of GPA is a tripartite structure: an NH_2-terminal domain pointing to the outside of the erythrocyte membrane, a transmembrane domain, and a COOH terminus located on the cytoplasmic face. In many systems, it has been suggested that association between single predicted transmembrane domains could play a key role in the mechanism of signal transduction by generating a high-affinity binding site for a ligand (Bormann et al., 1989). For example, T-cell receptor A and CD3W (Manolios et al., 1990; Cosson et al., 1991) have been proposed to associate to each other via a single transmembrane α-helix. For the epidermal growth factor receptor (EGFR), there is considerable evidence that ligand-induced receptor dimerization is the primary event in signaling (Ullrich & Schlessinger, 1990). Specific interactions between intramembraneous domains may provide part of the energy for this dimerization. A valine to glutamic acid mutation in the transmembrane domains of the neu oncogene product causes this EGFR-like molecule to become active (Bargmann et al., 1986) and increases the proportion of it found as dimer (Weiner et al., 1989). Therefore, the understanding of the dimer formation process should provide information about the ligand-induced signal transduction mechanism.

GPA has been shown to form a dimer stabilized via noncovalent association of its transmembrane domain (Furthmayr & Marchesi, 1976). Addition of a synthetic peptide corresponding to the GPA transmembrane domain disrupts the dimer, but addition of peptides corresponding to the transmembrane domain of unrelated proteins had no effect (Bormann et al., 1989). Binding of ligands to the extracellular domain of GPA induces a decrease in membrane deformability which is regulated by the skeletal proteins on the cytoplasmic side: this suggests that ligand binding may initiate a transmembrane signal (Chasis et al., 1988). A knowledge of the topology and the structure of the transmembrane domain is therefore a prerequisite for the understanding of oligomerization and signal transduction via the membrane domains of a protein. This information is available for a limited number of membrane proteins which were crystallized successfully (Michel, 1987). In the present study, purified glycophorin has been inserted into DMPC vesicles, and proteinase K (PK) has been used to cleave the domains protruding to the outside and/or the inside of the bilayer. The lipid-associated peptides were isolated and sequenced. ATR-FTIR was used to gain information about the secondary structure and orientation of glycophorin and its fragments into the lipid bilayer (Surewicz et al., 1993; Arrondo et al., 1993; Goormaghtigh & Ruysschaert, 1990). ATR-FTIR is especially recommended to study membrane proteins and has been successfully used in our laboratory to deal with membrane structural problems (Goormaghtigh et al., 1989, 1990, 1991a,b, 1993; Cabiaux et al., 1989; Vandenbussche et al., 1992). The topology of the GPA dimers is discussed in terms of existing models.

EXPERIMENTAL PROCEDURES

Reagents. L-α-Dimyristoylphosphatidylcholine (DMPC), phenylmethanesulfonyl fluoride (PMSF), and anti-glycophorin A antibody (αGP) were purchased from Sigma Chemical Co. (St. Louis, MO). Proteinase K (PK) and endoproteinase Glu-C were from Boehringer Mannhein; PVDF (Problott) membranes were obtained from Applied Biosystems, and acrylamide was from Bio-Rad. Outdated blood was a gift of Hôpital Saint Pierre (Brussels).

† This work was performed with the financial support of ARC (Actions de Recherches Concertées) and FNRS (Fonds National de la Recherche Scientifique). One of us (E.G.) is a Senior Research Associate of the National Fund for Scientific Research. We gratefully thank the Commission of the European Communities for continued financial support.

* Address correspondence to this author (telephone 32-2-6505377; Fax 32-2-6505113).

‡ Free University Brussels.

§ Smith Kline Beecham Biologicals.

® Abstract published in *Advance ACS Abstracts,* May 15, 1994.

[1] Abbreviations: GPA, glycophorin A; ATR, attenuated total reflection; FTIR, Fourier transform infrared spectroscopy; PK, proteinase K; DMPC, L-α-dimyristoylphosphatidylcholine; PMSF, phenylmethanesulfonyl fluoride; PVDF, polyvinylidene difluoride.

0006-2960/94/0433-6902$04.50/0

(*I*) *Purification of Glycophorin.* Glycophorin was isolated from erythrocyte ghosts prepared as described by Dodge et al. (1963) from recently outdated blood with no blood group preference. The sialoglycoprotein was isolated from lyophilized ghosts by suspending the dried membranes in a lithium diiodosalicylate solution and partitioning in a phenol–water mixture according to Marchesi and Andwers (1971). GPA isolated by this method consists mainly of a GPA dimer as judged by SDS–PAGE (Figure 2, lane 2) and immunoblotting with antibody against GPA (data not shown).

(*II*) *Incorporation of Glycophorin A into Vesicles.* Glycophorin was incorporated into lipid vesicles as described (Mac Donald & Mac Donald, 1975). A total of 225 volumes of a 2/1 (v/v) mixture of chloroform–methanol containing 5 mg of DMPC was mixed with 1 volume of a solution of glycophorin in distilled water (10 mg/mL) (GPA–lipid 1/5 w/w). The solvent was removed at 40–50 °C under N_2 flow, and the film was dried under vacuum overnight. This film was hydrated at 40 °C with 50 mM Tris-HCl and 5 mM $CaCl_2$, pH 7.6, buffer. The suspension was centrifuged at 125000*g* (Beckman ultracentrifuge) for 40 min at 4 °C. The supernatant containing free GPA was discarded, and the pellet was resuspended in 50 mM Tris-HCl and 5 mM $CaCl_2$, pH 7.6, buffer and 0.02% NaN_3 for further use.

(*III*) *Digestion.* (*a*) *External Digestion.* Glycophorin inserted into vesicles as described above was treated with proteinase K (PK–GPA 1/20 w/w) during 3 h at 37 °C. Digestion was stopped by addition of PMSF in ethanolic solution (3 mM final concentration). In an attempt to cleave glutamic acids 70 and 72 of GPA, the GPA-containing vesicles were treated with endoproteinase Glu-C (enzyme–GPA 1/20 w/w) during 19 h at 24 °C in 10 mM ammonium acetate, pH 4, buffer. Digestion was stopped by addition of PMSF (3 mM final concentration). In an other set of experiments, to facilitate the endoproteinase Glu-C action, the GPA-containing vesicles were treated with PK (3 h) and centrifuged at 125000*g* for 1 h at 4 °C to remove PK. The pellet was then resuspended in the pH 4 buffer (10 mM ammonium acetate) before treatment with the endoproteinase Glu-C. The digestion was also stopped by addition of PMSF.

(*b*) *Internal/External Digestion.* The protein–lipid film (1 and 5 mg, respectively) was hydrated with 1 mL of a 50 mM Tris-HCl and 5 mM $CaCl_2$, pH 7.5, buffer containing 5 mg of proteinase K. The vesicles were centrifuged at 125000*g* to remove the free GPA. As this purification step also removes the external proteinase K, the pellet was resuspended in the same buffer and proteinase K was added (PK–GPA 1/20 w/w). The digestion was stopped by addition of PMSF.

(*IV*) *Sucrose Gradient.* After proteolysis, for both sections IIIa and IIIb the peptides associated with the vesicles were separated from the proteolytic enzymes and from the released peptides by centrifugation on a linear sucrose density gradient in a Beckman L7 ultracentrifuge. The digested sample was mixed with 80% sucrose (1/1 v/v) layered on the bottom of the linear 30–5% sucrose gradient and centrifuged at 125000*g* for 15 h at 4 °C. The fractions of the gradient were collected from the bottom of the tubes. The phospholipid and protein distributions were measured by a choline dosage (Test combination phospholipids, Boehringer Mannheim Biochemia) and a Lowry test (Lowry et al., 1951). Fractions containing both lipids and proteins were pooled and dialyzed against distilled water during 3 days to remove the sucrose.

(*V*) *Delipidation.* The digested samples were lyophilized, solubilized with cold ethanol, and incubated during 30 min at 4 °C under agitation. The precipitated peptides were recovered by centrifugation (100000*g* for 1 h), and the DMPC-containing supernatant was discarded. No peptides were found in the supernatant as judged by either Tris–Tricine or 15% SDS–PAGE (data not shown).

(*VI*) *Gel Electrophoresis.* Small polypeptides were separated on a Tris–Tricine SDS–polyacrylamide gel (Schägger & von Jagow, 1987). A separating gel containing 16.5% T [T denotes the total percentage concentration of both monomers (acrylamide and bis(acrylamide))] and 6% C (C denotes the percentage concentration of the cross-linker relative to the total concentration) was used, overlaid by a 10% T, 3% C spacer gel and a 4% T, 3% C stacking gel. All samples were run in denaturing and reducing conditions in a 4% SDS, 12% glycerol (w/v), 50 mM Tris-HCl, 2% mercaptoethanol (v/v), and 0.01% bromophenol blue, pH 6.8, buffer. Electrophoresis was carried out at room temperature for about 20 h. SDS–polyacrylamide gels (Laemmli, 1970) with 4% stacking gel and 15% resolving gel were used to characterize the external digestion products of glycophorin-containing vesicles. The gels were stained either with Coomassie blue or with a silver staining method (Merril et al., 1983).

(*VII*) *Blotting and Sequencing.* After electrophoresis, the gels were immediately immersed into the cathode buffer (25 mM Tris, 192 mM glycine, 0.1% SDS). The PVDF (Problott) membrane (Mastudaira, 1987) was initially wetted with methanol before use and then equilibrated into the anode buffer (25 mM Tris, 192 mM glycine, 20% methanol). The peptides were transferred at 24 V during 2 h on the Problott membrane by a semidry blotting method, using Biometra Fast-Blot equipment. In every case, the gel was silver stained to assess that all the peptides present on the gel were transferred onto the membrane. The Problott membrane was stained with Coomassie blue to localize the bands. These bands were cut out, and the NH_2-terminal ends of the peptides were sequenced by Edman degradation on an Applied Biosystems 477A pulsed-liquid sequenator.

(*VIII*) *Fourier Transform Infrared Spectroscopy.* (*a*) *Methods.* Attenuated total reflection infrared (ATR-FTIR) spectra were obtained on a Perkin-Elmer 1720X FTIR spectrophotometer equipped with a liquid nitrogen cooled MCT detector. A total of 128 scans were averaged for each measurement. The internal reflection element is a germanium ATR plate (50 × 20 × 2 mm; Harrick EJ2121) with an aperture angle of 45° yielding 25 internal reflections. Measurements were carried out at room temperature. Thin films were obtained as described previously (Fringeli & Günthard, 1981). For polarization experiments, a Perkin-Elmer gold-wire polarizer was placed before the sample and before the reference plate. The ATR plate was sealed in a universal sample holder (Perkin-Elmer 186-0354) and deuterated by flushing (D_2O) saturated N_2 (room temperature) for 3 h when indicated. Upon H/D exchange, the absorption band associated with the random secondary structure shifts from about 1655 cm^{-1} to about 1642 cm^{-1}. This permits one to differentiate α-helical secondary structure from random secondary structure (Susi et al., 1967). To avoid recording spectra of material not included in the cavity of the universal sample holder, which has a controlled atmosphere, a 10-mm window was left open on the middle of the aperture of the ATR plate; the two side regions were masked by a thick Teflon sheet.

(*b*) *Secondary Structure Estimation.* The determination of the secondary structure of soluble and membrane proteins by analysis of the shape of the deuterated amide band has been described previously (Cabiaux et al., 1989; Goormaghtigh

& Ruysschaert, 1990; Goormaghtigh et al., 1990). The following frequencies were assigned to a given secondary structure: 1661–1647.5 cm^{-1}, α-helix; 1689–1682 and 1637.5–1615 cm^{-1}, β-sheet; 1644.5–1637.5 cm^{-1}, "random"; 1682–1661 cm^{-1}, "turns".

(*c*) *Orientation of the Secondary Structures.* The theory on the determination of molecular orientations by infrared ATR has been reviewed by Fringeli and Günthard (1981) and Goormaghtigh and Ruysschaert (1990) and will not be described in more detail here. When orientation was to be evaluated, spectra were recorded with parallel (0°) and perpendicular (90°) polarized incident light. Dichroism spectra are computed by subtracting the 0° polarized spectra from the 90° polarized spectra. A larger absorbance at 90° (upward deviation on the dichroism spectrum) indicates a dipole oriented preferentially near a normal to the ATR plate. Conversely, a larger absorbance at 0° (downward deviation on the dichroism spectrum) indicates a dipole parallel to the surface of the ATR place. The dipole associated to the ν-(C=O) (amide I) vibration is almost parallel to the C=O axis. In an α-helix, the main transition dipole moment lies close to parallel to the helix axis, while in an antiparallel β-sheet, it is predominantly perpendicular to the fiber axis.

(*d*) *Sample Preparation for Infrared Spectroscopy.* The GPA-containing vesicles were prepared as described by Mac Donald and Mac Donald (1975). The free and aggregated GPA was separated from the lipid-associated GPA by centrifugation on a linear 30–5% sucrose gradient. The digested samples were obtained as described in Experimental Procedures (sections IIIa and IIIb). The peptides associated to the vesicles after proteolysis were separated from the proteolytic enzymes and the released peptides by centrifugation on a linear sucrose density gradient (30–5%). In all cases the sucrose was removed by dialyzis (Pierce microdialyser). For each sample, the oriented multilayers were obtained as described by Fringeli and Günthard (1981) by evaporating 50–100 μL of the sample on one side of the ATR plate under a flux of nitrogen.

RESULTS

Digestion of the Inner and Outer Domains of GPA. To identify the transmembrane domain of GPA, GPA-containing liposomes were prepared and treated both from the inside and from the outside of the vesicles by proteinase K as described in Experimental Procedures (section IIIb). Proteolysis was stopped by addition of PMSF after a 3 h of digestion at 37 °C. The membrane-associated peptides were separated from the cleaved peptides and from the enzyme on a linear 30–5% sucrose gradient (see Experimental Procedures) (Figure 1). Free peptides or proteins remain at the bottom (data not shown). Fractions 13–15, containing both lipids and proteins (Figure 1), were pooled and dialyzed to remove the sucrose. Before being run on the polyacrylamide gel, the sample was delipidated to prevent the large amount of lipid from interfering with migration of the polypeptides. This sample was run on a Tris–Tricine SDS–PAGE (16.5% T, 6% C). A Coomassie blue staining weakly revealed the presence of protected peptides. Therefore, to increase the staining sensitivity, the gel was destained and stained with the silver staining method of Merril et al. (1983). In these conditions, a single band with an apparent molecular mass of 7.5 kDa was identified (Figure 2, land 3). On the same gel, GPA reconstituted in lipid vesicles and delipidated migrates with an apparent molecular mass of 66 kDa (Figure 2, lane 2), which indicates that the protein is present as a dimer in the lipid membrane.

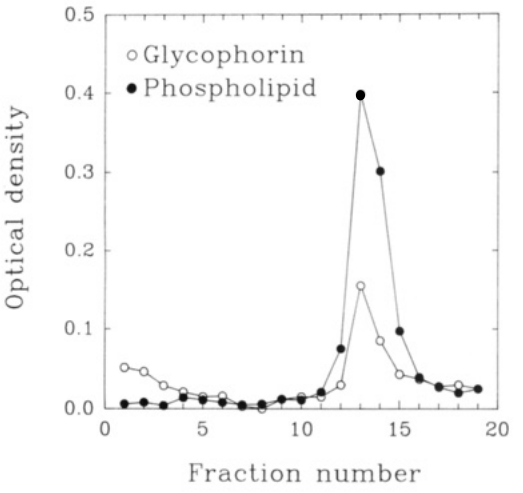

FIGURE 1: Sucrose gradient profiles of glycophorin-containing vesicles after cleavage by proteinase K from the outside and the inside of the vesicle (Experimental Procedures, section IIIb). After centrifugation 0.25-mL fractions were collected from the bottom to the top of the gradient and measured for protein and lipid content as described under Experimental Procedures.

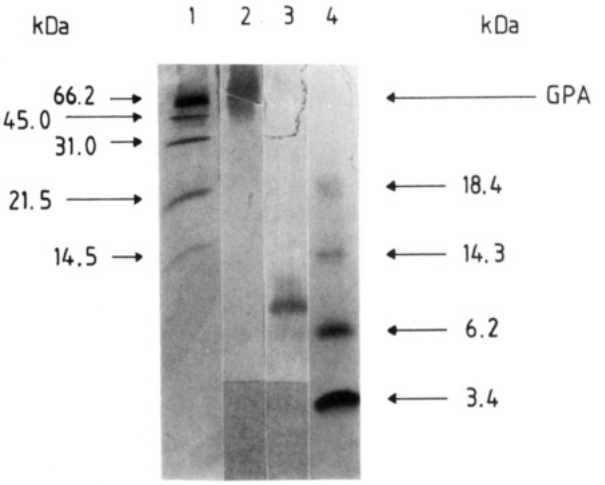

FIGURE 2: Tris–Tricine gel electrophoresis (16% T, 6% C) (Experimental Procedures). The gel was stained with the silver staining procedure. Lanes: 1, molecular mass markers (from top to bottom) bovine serum albumin, hen egg white ovalbumin, bovine carbonic anhydrase, soybean trypsin inhibitor, and hen egg white lysozyme; 2, undigested glycophorin-containing vesicles; 3, glycophorin-containing vesicles after cleavage by proteinase K from the outside and the inside of the vesicle; 4, low molecular weight markers (from top to bottom) β-lactoglobulin, lysozyme, bovine trypsin inhibitor, and insulin (β chain).

The complete sequence of the 7.5-kDa band, as determined by Edman degradation after transfer to a Problott membrane, extends from His^{66} to Ile^{95}: ^{66}H-H-F-S-E-P-E-I-T-L-I-I-F-G-V-M-A-G-V-I-G-T-I-L-L-I-S-Y-G-I^{95}. The calculated molecular mass of this peptide is 3.2 kDa. As no other sequence was identified, the 7.5-kDa band most probably contains a dimer of the identified peptide. It should be mentioned that when intact GP was treated with PK in the absence of lipid, no visible bands were detected on the gel (data not shown).

Digestion of GPA Outer Domains. The specificity of dimer formation is most probably mediated by a number of factors such as the topology of the nascent polypeptide chain in the erythrocyte membrane or the primary sequence, structure, and orientation of the transmembrane domain. To characterize the role played by the primary sequence of the transmembrane domain in dimer formation, GPA-containing vesicles were treated by a protease externally added to the

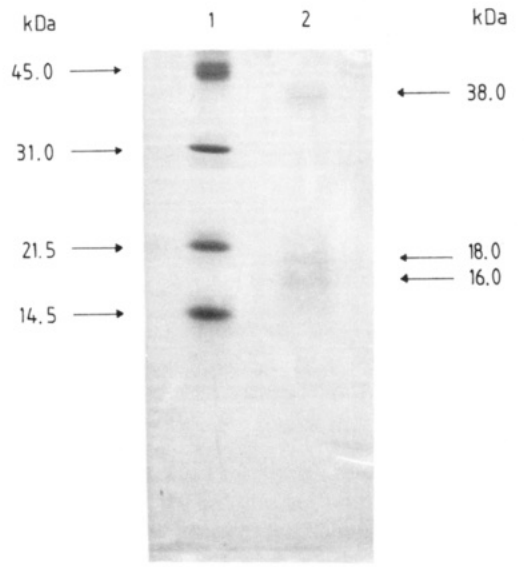

FIGURE 3: 15% SDS–polyacrylamide gel electrophoresis. The gel was stained with Coomassie blue. Lanes: 1, molecular masses; 2, external digestion of glycophorin-containing vesicles by proteinase K (see Experimental Procedures, section IIIa).

reconstituted system. This experiment was carried out according to section IIIa of Experimental Procedures. The GPA-containing vesicles were incubated with PK at 37 °C for 3 h. The proteolysis was stopped by addition of PMSF (3 mM final concentration). The membrane-associated peptides were separated from the cleaved peptides and the enzyme on a linear 30–5% sucrose gradient. The fractions of the gradient were analyzed for their lipid and protein content as in Figure 1. Fractions containing proteins and lipids were pooled and dialyzed to remove the sucrose. After delipidation, the fractions were analyzed by SDS–PAGE (15% acrylamide gel). The gel revealed the presence of two bands whose molecular masses were 16 and 38 kDa, respectively (Figure 3, lane 2). An 18-kDa band was also identified in this experiment, but it was most probably a partially digested form of the 16-kDa band since it disappeared in favor of this band after longer exposure to proteinase K (data not shown).

The molecular masses of the observed peptides were compared with the molecular masses of the peptides which would be obtained if "head to head", "head to tail", or "tail to tail" glycophorin dimers (Figure 4) were exposed to an externally added protease. On the basis of the amino acid and oligosaccharide composition and assuming that cleavage occurs at His^{66} and Ile^{95}, as demonstrated in the previous experiments, the external digestion would generate dimers of calculated molecular masses of 14.4, 36.2, and 58 kDa (Figure 4), respectively. The 16-kDa band (Figure 3, lane 2) suggests the presence in the sample of a dimer in a head to head configuration as illustrated in Figure 4A and the 38-kDa band (Figure 3, lane 2) of a head to tail dimer (Figure 4B). These two bands were transferred on a Problott membrane, and their N-terminal sequences obtained by Edman degradation are reported in Table 1. Two peptides starting respectively at His^{66} and Ser^{69} were identified in the 16-kDa band, which, assuming that this band contains a dimer, would correspond to a head to head dimer. The presence of a sequence starting at Ser^{69} that accounts for about 40% of the peptides present in the band suggests that either the His^{66} peptide is due to an uncomplete digestion or that one strand of the dimer (Ser^{69}) is shifted from three residues as compared to the other strand (His^{66}).

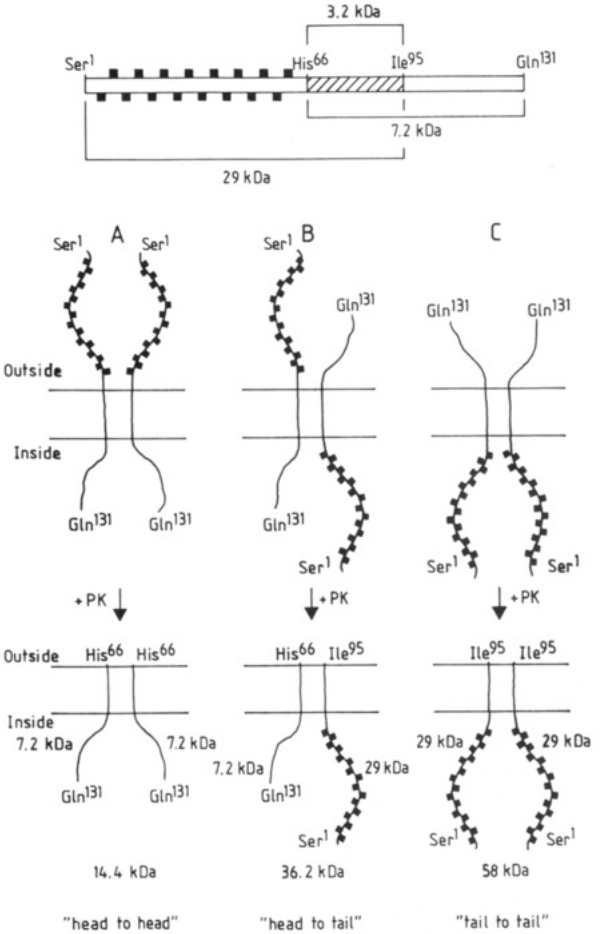

FIGURE 4: Schematic representation of the three possible modes of assembly of glycophorin A dimers inserted into vesicles of DMPC before and after outer digestion. The molecular masses of the three dimers as calculated from their estimated amino acids and oligosaccharide composition after digestion of the outer domain are 14.4, 34.2, and 58 kDa for A, B, and C, respectively. (■) Oligosaccharide chains.

In the 38-kDa band, two sequences starting at residues His^{66} and Ser^{1} were identified. This would be expected if an head to tail dimer was associated to the membrane (Figure 4B). These results suggest the presence of both a head to head and a head to tail configuration of GPA in the membrane before cleavage. The fact that we observed no band at 58 kDa allows us to exclude the formation of a tail to tail dimer oriented with the NH_2 terminus toward the inside of the vesicles, probably because of the large volume of the NH_2-terminal domain.

Digestion by Endoproteinase Glu-C. The NH_2-terminal domain of the membrane-associated peptide (His^{66}–Ile^{95}: 7.5 kDa, Table 1) contains four polar amino acids: two glutamic acids at positions 70 and 72 and two histidines at positions 66 and 67 that could be located outside the membrane and not be cleaved by proteinase K since this enzyme has been reported to cleave mainly at the level of the carboxylic group of aliphatic and aromatic amino acids (Ebeling et al., 1974). Therefore, the GPA-containing vesicles were treated with endoproteinase Glu-C (see Experimental Procedures, section IIIa), an enzyme which cleaves Glu residues in acidic conditions (pH 4) (Houmard & Drapeau, 1972). The membrane-associated peptides were purified on a linear 30–5% sucrose gradient. The sample was delipidated, run on SDS–PAGE (15% polyacrylamide gel), and transferred on a Problott membrane. Coloration of the membrane Problott with Coomassie blue reveals the presence of two bands of 18 and 40 kDa (data not shown). The NH_2-terminal sequence of the 18-kDa band

Table 1: NH_2-Terminal Sequence of Generated Peptides from Proteolytic Digestion of GPA-Containing Vesicles

	enzyme	app mol mass (kDa)	NH_2-terminal sequence
outer digestion[a]	PK	16	^{66}H-H-F-S-E-P-E-I-T-L-I-I-F-G-V-M-A-G-V-
			^{69}S-E-P-E-I-T-L-I-I-F-G-V-M-A-G-V-I-G-T-
		38	^{66}H-H-F-S-E-P-E-I-T-L-I-I-F-G-V-M-A-G-V-
			^{1}S-S-T-T-G-V-A-M-H-T-S-T-S-S-S-V-T-K-S-
	EndGlu	18	^{58}T-G-E-R-V-Q-A-H-H-F-S-E-P-E-I-T-L-I-I-
		40	sequence not determined
	PK + EndGlu	16	^{66}H-H-F-S-E-P-E-I-T-L-I-I-F-G-V-M-A-G-V-
			^{69}S-E-P-E-I-T-L-I-I-F-G-V-M-A-G-V-I-G-T-
		38	sequence not determined
inner and outer digestion[b]	PK	7.5	^{66}H-H-F-S-E-P-E-I-T-L-I-I-F-G-V-M-A-G-V-I-G-T-I-L-L-I-S-Y-G-I^{95}

[a] The GPA-containing vesicles were treated by a protease externally added to the reconstitution system as described in Experimental Procedures (section IIIa). [b] The GPA-containing vesicles were treated both from the inside and outside of the vesicles by PK as described in Experimental Procedures (section IIIb). Abbreviations: GPA, glycophorin A; PK, proteinase K; EndGlu, endoproteinase Glu-C.

yields Thr^{58} as the first amino acid (Table 1), which indicates that the Glu residues located downstream to that sequence (Glu^{70} and Glu^{72}) are not accessible to the enzyme. To facilitate the endoproteinase Glu-C action, the GPA-containing vesicles were first incubated with proteinase K, and endoproteinase Glu-C was added after elimination of proteinase K (section IIIa). The gel electrophoretic analysis revealed the presence of two peptides whose molecular masses (16 and 38 kDa; data not shown) are identical to those of the peptides identified when GPA-containing vesicles were treated only with the externally added proteinase K (Figures 3, lane 2), The 16-kDa band was transferred onto a Problott membrane. The sequence yields His^{66} and Ser^{69} as the first amino acids, which confirms that the external addition of either proteinase K or proteinase K + endoproteinase Glu-C generates an identical fragment with an apparent molecular mass of 16 kDa. This suggests that glutamic acids 70 and 72 are indeed protected from digestion either as a consequence of their intramembranous location or because they interact with the DMPC hydrophilic moiety at the lipid–membrane surface, rendering their digestion difficult. The 38-kDa band generated by the proteinase K + endoproteinase Glu-C digestion (data not shown) has not been sequenced and was assumed to be identical to the 38-kDa band identified in the presence of proteinase K alone (Figure 3, lane 2).

Structure and Orientation of the GPA Domains. Vibrational bands of protein and particularly the amide I band, ν(C=O), are sensitive to the secondary structure. The secondary structure of GPA inserted into lipid vesicles before and after treatment with PK was studied by ATR-FTIR. ATR-FTIR spectra of thin films of glycophorin reconstituted in DMPC liposomes show four defined maxima between 1800 and 1400 cm^{-1} (Figure 5, panel A, spectrum a). The lipid ν(C=O) is present at 1737 cm^{-1}, glycophorin amide I ν(C=O) and amide II are located at 1656 and 1545 cm^{-1}, respectively, and the DMPC $\delta(CH_2)$ is at 1468 cm^{-1}. Digestion of the protein by proteinase K externally added to the reconstituted system and separation of the vesicles from the protease and from the released soluble peptides yield spectrum b. When the protease is allowed to reach the inside of the vesicle in addition to the outside, spectrum c is obtained. In order to verify that proteinase K entrapped into vesicles did not interfere with the amide I region of the protein, proteinase K was encapsulated into vesicles in the absence of GPA. Free enzyme was removed as described for GPA-containing vesicles. The encapsulated enzyme represents less than 1% of the amide I area of GPA-containing vesicles treated by proteinase K on both sides of the vesicles (data not shown). Spectra of panel B were obtained after deuteration of the samples. Comparison of panel A and panel B shows that amide II is almost totally shifted toward about 1450 cm^{-1} for the sample containing the intact protein but not for the samples treated by the protease. The absence of shift upon deuteration might be related to a poor extent of H/D exchange, which is a further indication that the fragments remaining after proteinase K digestion are inserted into the lipid bilayer. It must be stressed that differential interaction of the digested and undigested sample with the ATR plate surface cannot explain differences in H/D exchange since in our experimental conditions (100-μg sample spread over 4 cm^2) less than 4% of the molecules are in contact with the germanium plate. The area of amide I relative to the area of the DMPC ν(C=O) is a measure of the protein/lipid ratio (Goormaghtigh et al., 1990) and can be used to evaluate the extent of the digestion. Integration as illustrated on Figure 5 (dashed area) indicates that 24% of the GPA residues remain associated to the DMPC vesicles when the digestion proceeds from the outside of the vesicles only and 17% of the residues remain associated to the DMPC vesicles when the digestion proceeds from both the outside and the inside of the vesicles.

Since amide I is sensitive to the secondary structure of the protein, we reported on Figure 6 the amide I′ region (deuterated samples) of the ATR-FTIR spectra of the purified protein in solution and of the membrane-associated protein (curves a and b). The spectra of the purified glycophorin and glycophorin reconstituted in DMPC liposomes are rather broad, indicating the presence of several secondary structures in the protein. Spectra c and d corresponding respectively to the membrane-associated peptide resulting from the outside digestion in DMPC vesicles and to the membrane-associated peptide resulting from the outside and inside digestion are much sharper, with a maximum at 1656 cm^{-1} characteristic of the α-helix structure and a distinct shoulder near 1635 cm^{-1} which could be related to the presence of β-sheet. The shape of the amide I′ after cleavage of the external and internal glycophorin domain reveals a significant increase in helical content.

Polarized ATR-FTIR spectroscopy yields information as to the orientation of the phospholipids and of the protein secondary structures in thin films (Goormaghtigh et al., 1989, 1991a,b). Dichroism spectra obtained by subtracting a 0° polarized spectrum from a 90° polarized spectrum (Goormaghtigh et al., 1990) are reported in Figure 7 for the membrane-associated peptides resulting from the digestion of glycophorin reconstituted in DMPC vesicles from the outside (spectrum a) and from the outside and the inside of the vesicle (spectrum b). The dichroic spectrum presents a typical positive deviation on the high-frequency side of the ν(C=O) band at 1745 cm^{-1} (Figure 7). These stretching modes have been used by Mendelsohn et al. (1984) for mapping preferences

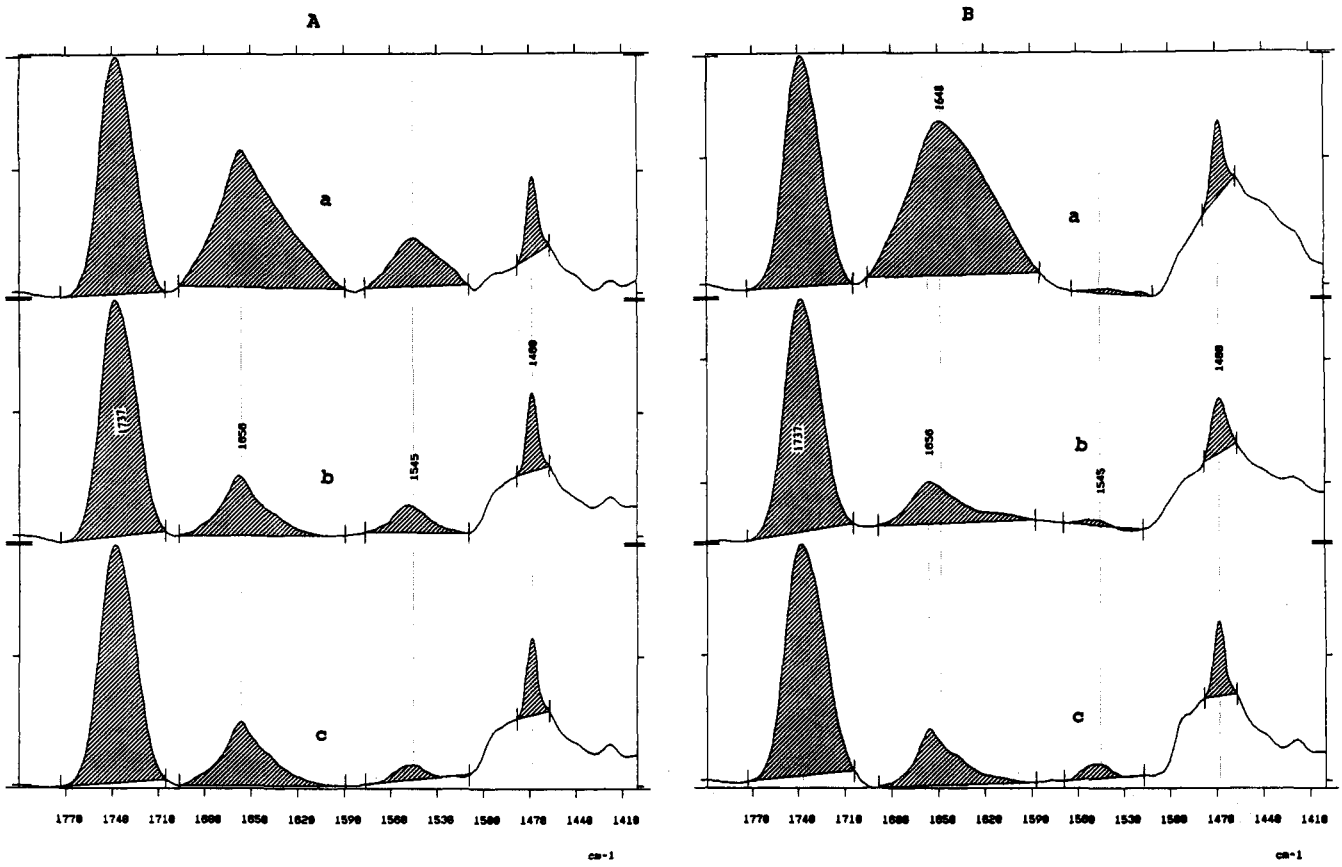

FIGURE 5: ATR Fourier transform infrared spectra between 1800 and 1400 cm^{-1} of glycophorin reconstituted into DMPC vesicles (curves a), of reconstituted proteoliposomes digested by proteinase K from the outside of the vesicle (curves b), and of reconstituted proteoliposomes digested by proteinase K from the outside and from the inside of the vesicle (curves c) (see Experimental Procedures). Spectra of the undeuterated samples are reported on panel A, and spectra of the deuterated samples are reported on panel B. Integrated areas between 1773–1705, 1692–1587, 1570–1516, and 1478–1457 cm^{-1} (panel A) and between 1773–1705, 1692–1587, 1570–1516, and 1478–1457 cm^{-1} (panel B) are hatched. Vertical dotted lines are at 1737, 1656, and 1468 cm^{-1} (panel A) and at 1737, 1656, 1648, and 1468 cm^{-1} (panel B). The scale has been adjusted so that the lipid ν(C=O) band at 1737 cm^{-1} has the same area on the figure. The actual amplitudes of the amide I spectra are as follows: for panel A, spectrum a, 0.226, spectrum b, 0.330, and spectrum c, 0.297; for panel B, spectrum a, 0.272, spectrum b, 0.347, and spectrum c, 0.253.

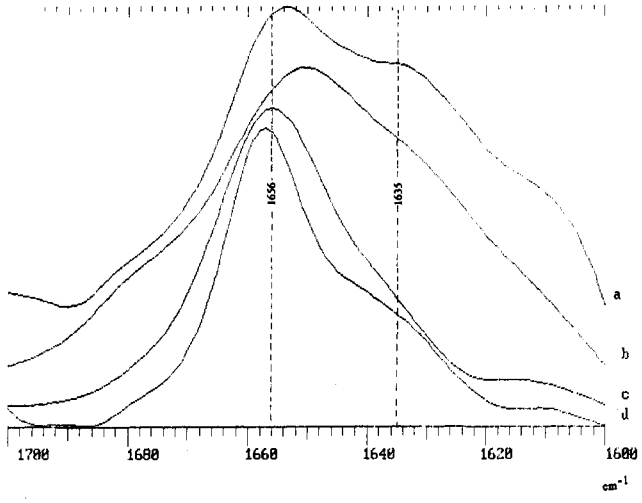

FIGURE 6: Comparison of the shape of amide I between 1700 and 1600 cm^{-1} for purified glycophorin (spectrum a), for glycophorin reconstituted into DMPC vesicles (spectrum b), after digestion of the reconstituted proteoliposomes by proteinase K from the outside of the vesicle (spectrum c), and after digestion of the reconstituted proteoliposomes by proteinase K from the outside and from the inside of the vesicle (spectrum d) (see Experimental Procedures).

between lipids and glycophorin. The $\delta(CH_2)$ band at 1468 cm^{-1} whose dipole is oriented perpendicular to the lipid acyl chains shows a negative deviation, and the $\gamma_w(CH_2)$ progression at 1200 cm^{-1} whose dipole is oriented parallel to the lipid acyl chains presents a clear positive deviation from the baseline (data not shown). These different features are in good agreement with our knowledge of the organization of phospholipid bilayers on the germanium crystals. Figure 7 shows that the maxima of the dichroism spectra are located at 1654 and 1658 cm^{-1} for the membrane-associated peptides (spectra a and b, respectively), which indicate that the observed dichroism is mainly due to the α-helical component of this peptide. A dichroic ratio of 2.2 and 2.1 was found for the digested samples (spectra a and b, respectively), which suggests a transmembrane orientation of the α-helical component, the helix axis being parallel to the lipid acyl chains. As already described for several transmembrane-oriented peptides, the α-helical band is located at slightly higher frequencies for the 90° polarization (1657 cm^{-1}) than for the 0° polarization (1655 cm^{-1}) as shown in Figure 8 where the polarized (90° and 0°) spectra of the sample cleaved from both sides of the membrane were rescaled to the same amplitude and superimposed. The reason for this shift has been discussed elsewhere (Goormaghtigh et al., 1991). In agreement with the transmembrane orientation of the helix component, the amide II band at 1549 cm^{-1} which can be assigned to the unexchanged helices looks more intense for the 0° polarization than for the 90° polarization (Figure 8). The β-sheet orientation of the transmembrane fragment of GPA left after internal and external proteolytic digestion with respect to the lipid membrane cannot be safely inferred from the dichroic spectra

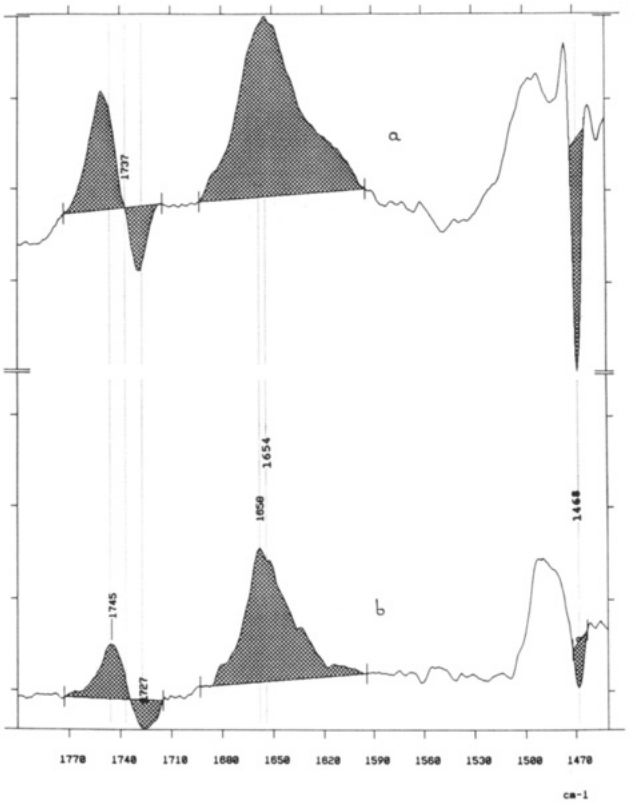

FIGURE 7: Dichroism spectrum of deuterated (5 h) glycophorin reconstituted into DMPC vesicles after digestion by proteinase K from the outside (spectrum a) and from the outside and the inside of the vesicle (spectrum b). The dichroism spectra were obtained by subtraction of its 0° polarized spectrum from its 90° polarized spectrum.

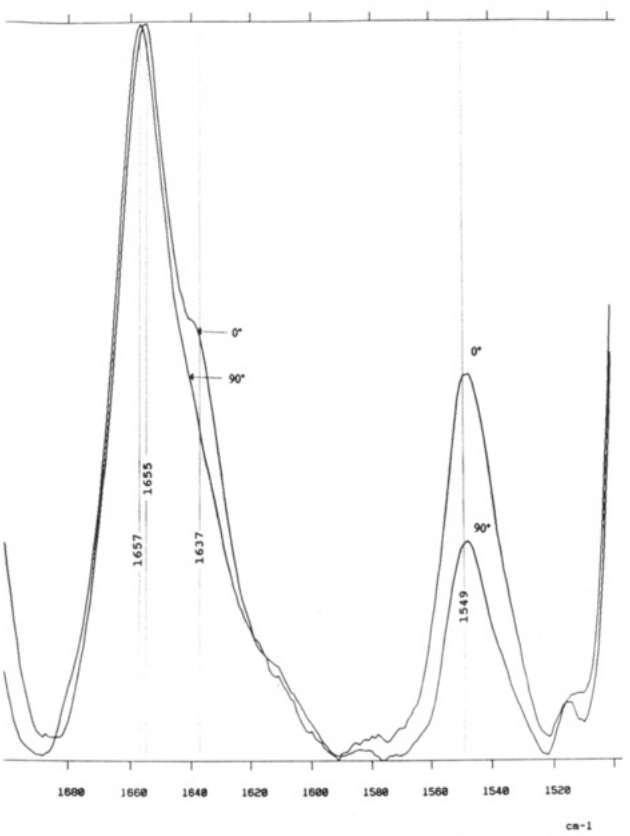

FIGURE 8: Polarized ATR–FTIR spectra of deuterated (5 h) glycophorin reconstituted into DMPC vesicles after digestion by proteinase K from the outside and the inside of the vesicle. Spectra are normalized to the same amide I intensity. Vertical dotted lines are located at 1657, 1655, 1637, and 1549 cm^{-1}.

reported on Figure 7b. However, as far as the β-sheet component is concerned, Figure 8 shows that a clear additional intensity appears between 1640 and 1620 cm^{-1} on the 0° polarized spectra. This indicates a preferential orientation of the carbonyl groups in the β-sheet structure parallel to the plane of the lipid membrane. This suggests that the β-sheet axis could be either parallel to the plane of the membrane, the structure lying at the surface, or perpendicular to the plane of the membrane, as could be expected for a transmembrane orientation.

DISCUSSION

Selective photolabeling of the hydrophobic core of red cell blood membranes revealed that the trypsin-insoluble peptide "Tis" (Val^{62}–Ile^{95}) contained most of the radiolabel associated to glycophorin A (Brunner & Semenza, 1981; Kahane & Gitlert, 1978). Photolysis of glycophorin vesicles containing phospholipids with photoactivable probes in their polar heads provided information about the probable boundaries of the membrane-embedded segment of glycophorin A (residues 62–96) (Ross et al., 1982). In this context, Ross et al. (1982) proposed a model where the 62–96 fragment is assumed to be helical and to span the 45 Å thick lipid bilayer. The presence of Pro^{71} would introduce a kink of 20° in the helix which allows the number of amino acids inserted into the lipid bilayer to increase (Ross et al., 1982).

Our data provide evidence that insertion of glycophorin A into DMPC vesicles protects the His^{66}–Ile^{95} domain from proteinase K digestion, either because it is completely inserted into the lipid bilayer or because one part of it interacts with the lipids at the membrane–water interface, rendering its digestion difficult. The analysis of the primary sequence of the His^{66}–Ile^{95} suggests that, on the basis of their relative unpolar character, residues 73–95 could be protected from digestion by being embedded in the membrane. The presence of a cleavage site at Ile^{95} which is accessible only for the protease encapsulated in the vesicles strongly supports this hypothesis. If we consider that the insertion of charged residues in the membrane could be energetically unfavorable, residues 66–73 or 69–73 are probably associated to the surface of the bilayer in such a way that they cannot be cleaved by PK. Components of amide I′ revealed by Fourier self-deconvolution were evaluated by a least-squares iterative curve fitting between 1600 and 1700 cm^{-1} (Cabiaux et al., 1989). The 66–95 peptide resulting from digestion of GPA on both sides of the DMPC vesicles contains 66% α-helix and 34% β-sheet (data not shown). This result indicates that two-thirds of the membrane-associated peptide adopts an α-helical structure which is long enough to span the membrane. Moreover, the orientation data clearly demonstrate that the helix axis is parallel to the lipid acyl chain. Therefore, we propose that residues 73–95 adopt a transmembrane helical topology. The data concerning the β-sheet domain are less straightforward to interpret. On the basis of secondary structure determination, about 10 residues would adopt a β-sheet conformation. These residues could correspond to the NH_2-terminal sequence of the PK-resistant peptide. The polarization data do not allow us to propose an single orientation of the β-sheet structure. However, because of the presence of charged residues in the sequence, we would rather favor a model in which the β-sheet lies at the surface of the lipid vesicles. Therefore, our proteolytic and spectroscopic data are in agreement with a topological model with the His^{66}–

Glu[72] peptide oriented parallel to the lipid–water interface and the transmembrane Ile[73]–Ile[95] domain oriented parallel to the lipid acyl chains. Treutlein et al. (1992) recently found that the glycophorin A membrane domain can be modeled as a right-handed supercoil helix. However, this type of structure has not yet been characterized by FTIR. We are therefore not able to interpret our data in terms of the presence or absence of a supercoiled helix. However, one should keep in mind that the frequency domain attributed to a helical structure covers a family of helices which may contain the right-handed supercoil helix.

The dimer formation specificity is of importance in the signal transduction mechanism. Addition of a synthetic peptide corresponding to the transmembrane domain of GPA disrupts the GPA dimers, whereas addition of peptides corresponding to the transmembrane domains of glycophorin C and interleukin 2–receptor Tac antigens did not affect the glycophorin dimer stability (Bormann et al., 1989). Moreover, Lemmon et al. (1992a) fused the glycophorin transmembrane domain with the COOH terminus of staphylococcal nuclease. The resulting chimera forms a dimer in SDS which is disrupted upon addition of a peptide corresponding to the GPA transmembrane segment. No effect was detectable with transmembrane domains of human neu oncogene, epidermal growth factor receptors, and helix α of bacteriorhodopsin (Lemmon et al., 1992a). These data strongly suggest that specific structural features of the GPA transmembrane domain mediate the dimer formation.

Our data provide evidence that head to head (Figure 4A corresponding to the 16-kDa band) and head to tail (Figure 4B corresponding to the 38-kDa band) dimers are formed between GPA molecules into the membrane of DMPC vesicles. We assumed, as demonstrated by Bormann et al. (1989), that dimers do not dissociate and reassociate randomly during electrophoresis. The absence of a 58-kDa band (Figure 3C) supports this hypothesis. It is likely that the head to tail interaction does not occur in the erythrocyte membrane, but the existence of such dimers in our reconstituted system raises questions about the conditions that must be fulfilled to allow their formation. Stability of such head to tail dimers even in the presence of SDS at 100 °C suggests that the specificity of the primary sequence in the GPA dimer formation should be reconsidered. Indeed, the hydrophobicity or steric hindrance of amino acid side chains may be more important for dimer formation than the nature of the residues. Lemmon et al. (1992b) showed, using mutational analysis, that subtle changes in the amino acid side-chain structures at sensitive positions disrupt the helix–helix association in the transmembrane domain of glycophorin A. The most sensitive positions are located approximately every 3.9 residues along the axis, which suggests that it is the helical structure which is involved in the dimer formation. This is in agreement with the model of Treutlein et al. (1992) in which a pair of helices are interacting via a right-handed supercoil formation. The role of the β-sheet structure observed in our experiments could be to stabilize the dimer. For a given side chain, the effect of mutations on dimerization depends on its position in the transmembrane sequence, and G79 and G83 seem to play a crucial role in the dimer formation. Indeed, all substitutions of G83 disrupt the dimers completely as does substitution of G79 with any residue other than alanine (Lemmon et al., 1992b). Using a simulated annealing technique, the two residues were proposed to be the closest point of contact between the two helices because of their small side chains (Treutlein et al., 1992). The central position of G83 in the transmembrane domain could explain the formation of head to tail dimers observed in our work. Indeed, it is conceivable that in a head to head dimer the G83 residues interact with the same residue on the second strand, whereas in a head to tail dimer G86 would interact with G83 and vice versa. This preferential interaction between glycine residues would in both cases be involved in dimer formation. It would be interesting to use the simulated annealing technique to demonstrate that the two helices oriented in the head–tail conformation are right-handed supercoils as calculated by Treutlein et al. (1992) for the head to head conformation.

From a more general point of view, most transmembrane regions have been shown to adopt an α-helical structure [e.g., the photosynthetic complex of *Rhodopseudomonas viridis* (Michel, 1987) and bacteriorhodopsin (Henderson et al., 1990)] even though an increasing number of membrane proteins are shown to adopt a β-sheet topology (Walian & Jap, 1990; Cowan et al., 1992; Weiss et al., 1991). Recently, part of the transmembrane sequence of the nicotinic acetylcholine receptor was found to contain β-sheet in a 9-Å resolution structure (Unwin et al., 1993). This was confirmed by FTIR (Görne-Tschelnokow, 1994). However, information about the structure exists only for a limited number of membrane proteins or is based on nonconvincing predictive approaches (Wallace et al., 1986). We have therefore combined a proteolytic approach and the advantages of the IR-ATR methodology to study more systematically the structure and orientation of a protein in a lipid bilayer. This approach has been applied here to GPA as a model system but should be extended to other membrane proteins with a single transmembrane domain in order to elucidate, on an experimental basis, the way the transmembrane domains accommodate the lipid environment and assemble to transduce information to the cytoplasmic domain.

REFERENCES

Arrondo, J. L. R., Muga, A., Castresana, J., & Gõni, F. M. (1993) *Prog. Biophys. Mol. Biol. 59*, 23–56.

Bargmann, C. I., Hung, M. C., & Weinberg, R. A. (1986) *Cell 45*, 649–657.

Bormann, B.-J., Knowles, W. J., & Marchesi, V. T. (1989) *J. Biol. Chem. 264*, 4033–4037.

Brunner, J., & Semenza, G. (1981) *Biochemistry 20*, 7174–7182.

Cabiaux, V., Brasseur, R., Wattiez, R., Falmagne, P., Ruysschaert, J.-M., & Goormaghtigh, E. (1989) *J. Biol. Chem. 264*, 4928–4938.

Chasis, J. A., Reid, M. E., Jensen, R. H., & Mohandas, N. (1988) *J. Cell Biol. 107*, 1351–1357.

Cosson, P., Lankford, S. P., Bonifacino, J. S., & Klausner, R. D. (1991) *Nature 351*, 414–416.

Cowan, S. W., Schirmer, T., Rummel, G., Steiert, M., Ghosh, R., Pauptit, R. A., Jansonius, J. N., & Rosenbusch, J. P. (1992) *Nature 358*, 727–733.

Dodge, J. T., Mitchell, C., & Hanahan, D. J. (1963) *Arch. Biochem. Biophys. 100*, 119–130.

Ebeling, W., Hennrich, N., Klockow, M., Metz, H., Orth, H. D., & Lang, H. (1974) *Eur. J. Biochem. 47*, 91–97.

Fringeli, U. P., & Günthard, H. H. (1981) in *Membrane Spectroscopy* (Grell, E., Ed.) pp 270–332, Springer-Verlag, Berlin.

Furthmayr, H., & Marchesi, V. T. (1976) *Biochemistry 15*, 1137–1144.

Goormaghtigh, E., & Ruysschaert, J.-M. (1990) in *Molecular description of biological membranes by computer aided conformational analysis* (Brasseur, R., Ed.) Vol. I, pp 285–329, CRC Press Inc., Boca Raton, FL.

Goormaghtigh, E., Martin, I., Vandenbranden, M., Brasseur, R., & Ruysschaert, J.-M. (1989) *Biochem. Biophys. Res. Commun. 158*, 610–616.
Goormaghtigh, E., Cabiaux, V., & Ruysschaert, J.-M. (1990) *Eur. J. Biochem. 193*, 409–420.
Goormaghtigh, E., De Meutter, J., Cabiaux, V., Szoka, F., & Ruysschaert, J.-M. (1991a) *Eur. J. Biochem. 195*, 421–429.
Goormaghtigh, E., Vigneron, L., Knibiehler, M., Lazdunski, C., & Ruysschaert, J.-M. (1991b) *Eur. J. Biochem. 202*, 1299–1305.
Goormaghtigh, E., Cabiaux, V., De Meutter, J., Rosseneu, M., & Ruysschaert, J.-M. (1993) *Biochemistry 32*, 6104–6110.
Görne-Tschelnokow, U., Strecker, A., Kaduk, Ch., Naumann, D., & Hucho, F. (1994) *EMBO J. 13*, 338–341.
Henderson, R., Baldwin, J. M., Ceska, T. A., Zemlin, F., Beckmann, E., & Downing, K. H. (1990) *J. Mol. Biol. 213*, 899–929.
Houmard, J., & Drapeau, G. R. (1972) *Proc. Natl. Acad. Sci. U.S.A. 69*, 3506–3509.
Kahane, I., & Gitlert, C. (1978) *Science 201*, 351–352.
Laemmli, U. K. (1970) *Nature 227*, 680–685.
Lemmon, M. A., Flanagan, J. M., Hunt, J. F., Adair, B. D., Bormann, B.-J., Dempsey, Ch. E., & Engelman, D. M. (1992a) *J. Biol. Chem. 267*, 7683–7689.
Lemmon, M. A., Flanagan, J. M., Treutlein, H. R., Zhang, J., & Engelman, D. M. (1992b) *Biochemistry 31*, 12719–12723.
Lowry, O. H., Rosebrough, N. J., Farr, A. L., & Randall, R. J. (1951) *J. Biol. Chem. 193*, 265–275.
Mac Donald, R. I., & Mac Donald, R. C. (1975) *J. Biol. Chem. 250*, 9206–9214.
Manolios, N., Bonifacino, J. S., & Klausner, R. D. (1990) *Science 249*, 274–277.
Marchesi, V. T., & Andwers, E. P. (1971) *Science 174*, 1247–1248.
Mastudaira, P. (1987) *J. Biol. Chem. 262*, 10035–10038.
Mendelsohn, R., Dluhy, R. A., Crawford, T., & Mantsch, H. H., (1984) *Biochemistry 23*, 1498–1504.
Merril, C. R., Goldman, D., & Van Keuren, M. L. (1983) *Methods Enzymol. 96*, 230–239.
Michel, H. (1987) *J. Mol. Biol. 158*, 567–572.
Ross, A. H., Radhakrishnan, R., Robson, R. J., & Khorana, H. G. (1982) *J. Biol. Chem. 257*, 4152–4161.
Schägger, H., & von Jagow, G. (1987) *Anal. Biochem. 166*, 368–379.
Surewicz, W. K., Mantsch, H. H., & Chapman, D. (1993) *Biochemistry 32*, 389–394.
Susi, H., Timasheff, S. N., & Stevens, L. (1967) *J. Biol. Chem. 242*, 5460–5466.
Tomita, M., Furthmayr, H., & Marchesi, V. T. (1978) *Biochemistry 17*, 4756–4770.
Treutlein, H. R., Lemmon, M. A., Engelman, D. M., & Brünger, A. T. (1992) *Biochemistry 31*, 12726–12733.
Ullrich, A., & Schlessinger, J. (1990) *Cell 61*, 203–212.
Unwin, N. (1993) *J. Mol. Biol. 229*, 1101–1124.
Vandenbussche, G., Clercx, A., Clercx, M., Curstedt, T., Johansson, J., Jörnvall, H., & Ruysschaert, J. M. (1992) *Biochemistry 31*, 9169–9176.
Walian, P. J., & Jap, B. K. (1990) *J. Mol. Biol. 215*, 429–438.
Wallace, B. A., Cascio, M., & Hielke, D. L. (1986) *Proc. Natl. Acad. Sci. U.S.A. 83*, 9423–9427.
Weiner, D. B., Liu, J., Cohen, J. A., Williams, W. V., & Greene, M. I. (1989) *Nature 339*, 230–231.
Weiss, M. S., Abele, U., Weckesser, W., Schiltz, E., & Schulz, G. E. (1991) *Science 254*, 1627–1630.